A 56CH MEMS MICROPHONE ARRAY FOR MEASURING WALL PRESSURE FLUCTUATION FIELD

Yoshitsugu Naka
Department of Mechanical Engineering
Meiji University
1-1-1 Higashimita Tama-ku Kawasaki Kanagawa, 214-8571, Japan
naka@meiji.ac.jp

Atsuki Miyajima
Department of Mechanical Engineering
Graduate School of Science and Technology
Meiji University
1-1-1 Higashimita Tama-ku Kawasaki Kanagawa, 214-8571, Japan
ce182056@meiji.ac.jp

ABSTRACT

The present study aims to develop a 56ch MEMS microphone array for turbulent wall pressure fluctuation measurement. 56 microphones are controlled by a FPGA, and the microphones are arranged in line to obtain spanwise distributions of the wall pressure fluctuations in a turbulent boundary layer. Output data of the MEMS microphones are converted to the actual pressure fluctuations based on the calibration using a reference microphone. The background noise in the wind-tunnel is reduced by splitting the data into POD modes. The noise-reduced data are reconstructed by excluding the modes containing significant amount of noise. The normalized RMS values of the wall pressure fluctuations are in good agreement with the data in the literature, and the power spectra show smooth curves down to the wall unit frequency. Two-dimensional fluctuating wall pressure field and the two-point correlation of fluctuating wall pressure indicate contributions of the turbulent flow structures. The present method can be extended to build a massively parallel fluctuating pressure measurement system.

INTRODUCTION

There have been a number of efforts to reveal the relationship between the wall pressure fluctuations and the structures of wall turbulence. It has not yet been fully revealed that the wall pressure fluctuations contain how much contributions from the turbulence structures above. Naka *et al.* (2015) evaluated the three dimensional shape of the wall pressure–velocity correlations in a turbulent boundary layer, and it is confirmed that the wall pressure fluctuations include the contributions from the outer layer. To further understand the link between the wall pressure fluctuations and the turbulence structures, measurements of the time resolved wall pressure fluctuation field are desired. Matsubara *et al.* (2014) evaluated the effect of the tripping on wall pressure–velocity correlations using a 32ch microphone array. White *et al.* (2012) manufactured a 64ch microphone array using micro machining technique applying it to the measurement in a turbulent boundary layer. To date, however, the wall pressure fluctuation measurements reported have been restricted in relatively small number of sensors with the insufficient spatial dynamic range. In the present study, a flexible microphone array system for many channel pressure fluctuation measurements is proposed, and the applicability of the technique is examined.

A MICROPHONE ARRAY FOR WALL PRESSURE FLUCTUATION MEASUREMENT

For sensing turbulent pressure fluctuations, a digital miniature MEMS microphone (INMP621, InvenSense) is used. The maximum input pressure fluctuation is 133 dB-SPL (89.3 Pa RMS). This microphone has the signal to noise ratio of 65 dB. That gives the minimum sensible pressure fluctuation level of 5.64×10^{-4} Pa RMS. The frequency range giving flat amplitude response is from 45 Hz to 20 kHz. The dimension is $4\times3\times1$ mm, and it has a pressure port with the diameter of 0.25 mm in the bottom surface. The wiring of this microphone is accomplished by surface mount soldering.

Figure 1 shows the microphone array designed for the present measurement. The dimension of the array board is 100×160 mm. Since the microphone has its port on the bottom side, holes with the diameter of 0.5 mm are manufactured. The microphones are implemented in two rows, and each row has 28 microphones. The distance between two rows Δx is 3 mm and the distance between adjacent microphones in the row Δz is 4 mm. The second row is shifted 2 mm in z direction against the first one so that the apparent spanwise spatial resolution can be increased. The opposite side of the board is flat and works as a part of the wall.

A FPGA board (ZYBO Zynq-7000, digilent) is used for controlling microphones. The board has four PMOD (Peripheral Module) connectors available for communicating with microphones. Each PMOD connector has 12 pins. Four pins are taken for the power supply and the ground. One pin is designated for sending the 2.5 MHz reference

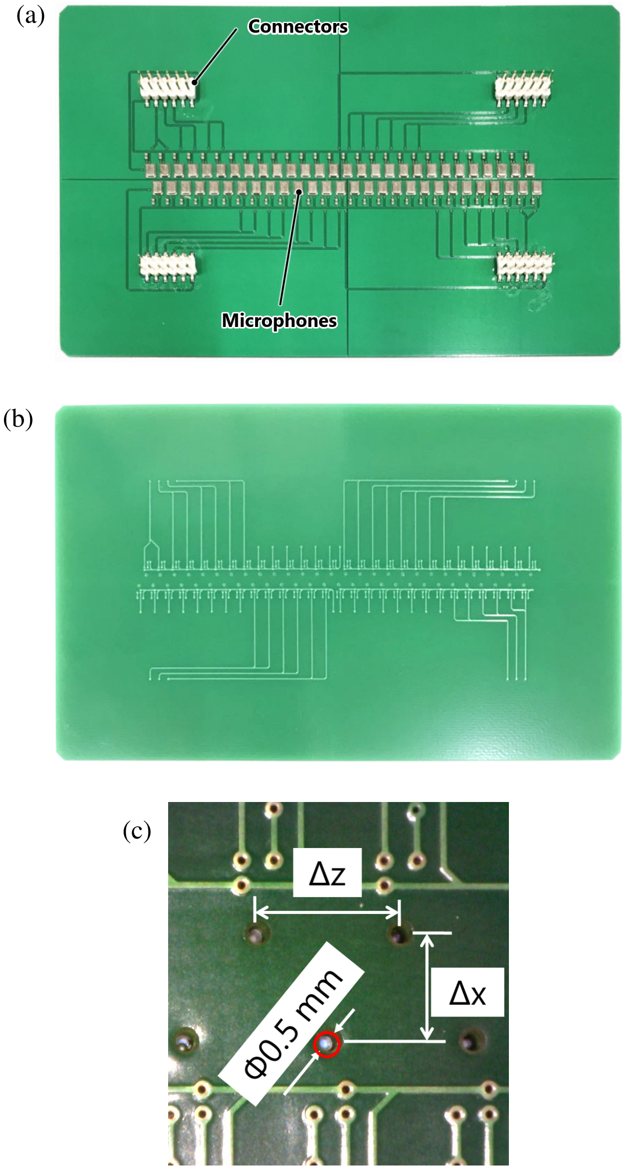

Figure 1. Photos of the microphone array: (a) mounted side, (b) hole side, (c) enlarged view of holes.

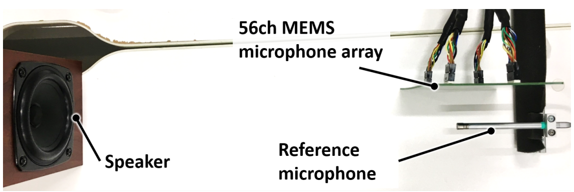

Figure 2. Setup for the frequency response calibration.

clock pulse signal obtained by 40 division of 100 MHz base clock of the FPGA. Seven pins receive the signal from microphone synchronized to the reference clock. High and low levels of the reference clock signal corresponds to left and right channels of the microphone, respectively. Therefore, signals from the two microphones can be handled with one pin. One PMOD connector has 14 pins, and 56 microphones can be controlled by a ZYBO board. It is noted that the present system can be readily extended if multiple boards are prepared. Synchronization can be achieved using

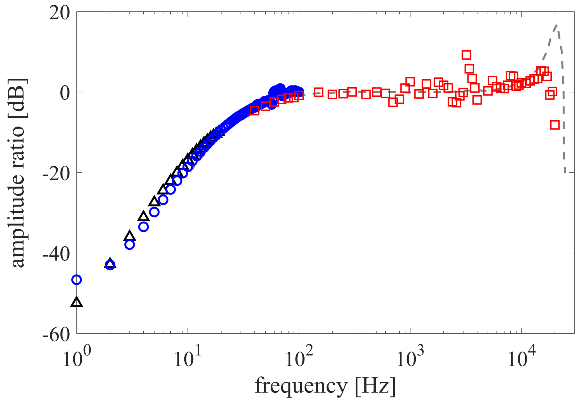

Figure 3. Amplitude response; low-frequency response measured by the reference microphone (circle), low-frequency response measured by the pressure transducer (triangle), mid- to high-frequency response (square) and response of the microphone provided by manufacturer (dashed line).

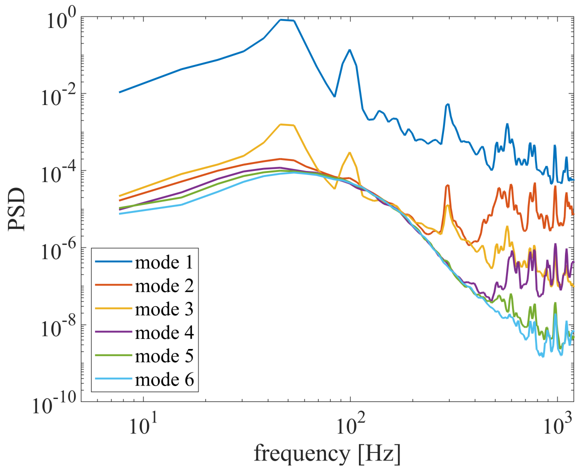

Figure 4. Power spectra of the first six POD modes.

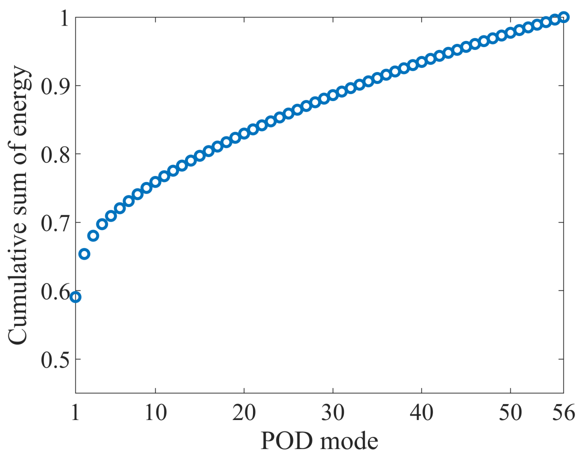

Figure 5. POD mode versus energy component.

external triggering.

Output data from microphones are 1-bit PDM (pulse density modulated) signals. Data from the 56 microphones are packed into 32 bit data stream by the ZYBO board and written into the disk. The bundled bit stream data are de-

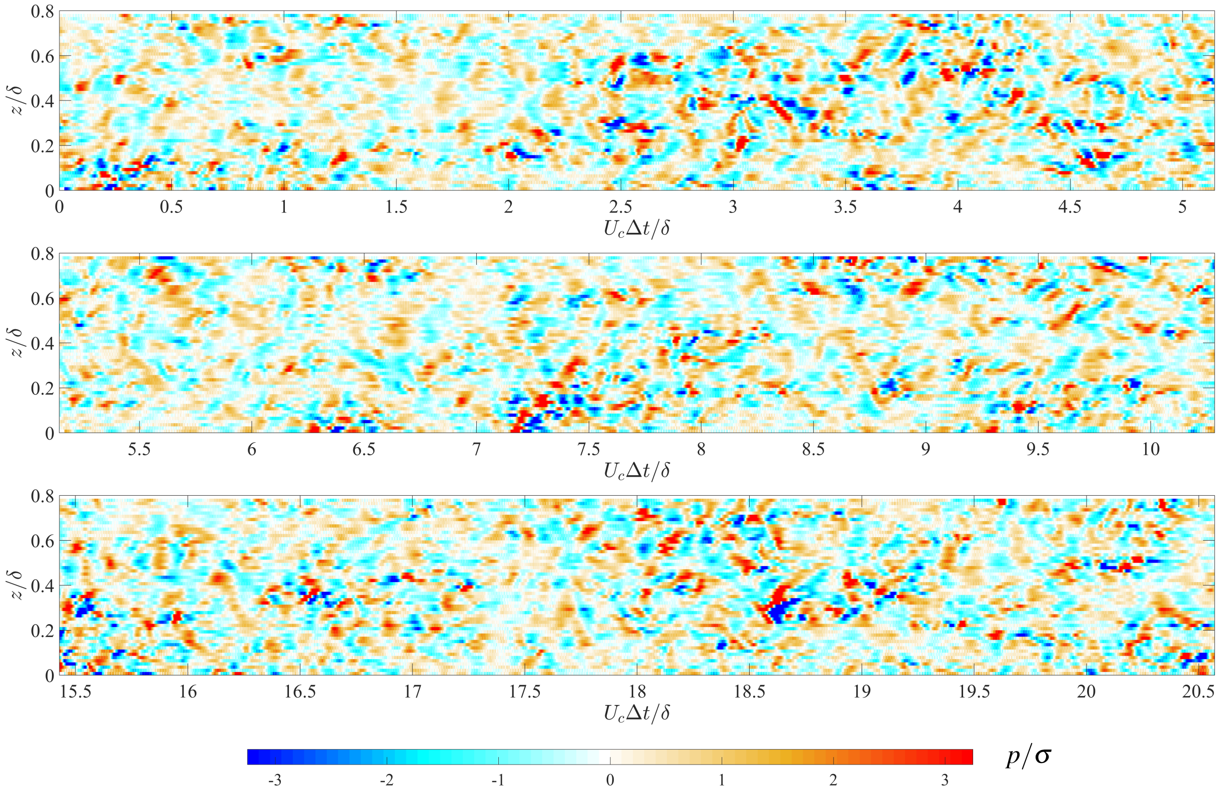

Figure 6. Reconstructed space-time distribution of fluctuating pressure.

coded off-line by the zero-phase shift digital sinc^2 filter with the width of 64. After waveform of the pressure signal is recovered, the 2.5 MHz signal is decimated to 125 kHz.

The amplitude of the microphone output signal is converted into the actual pressure fluctuations in Pascal based on the calibration. The calibration measurement has been performed as the microphone array is placed close to the reference microphone (4938-A-011, B&K). The setup of the calibration measurement is presented in Fig. 2. The tonal signals from a speaker are recorded simultaneously by the microphone array and the reference microphone. For the low frequency range namely below 20 Hz, the pressure transducer (Valydine DP45, and PA701) was also employed. In this measurement, the microphone array, a pressure port for the transducer and a speaker were attached to the inner wall of a closed box, and the pressure fluctuation in the box was measured.

The amplitude response of the microphone array is shown in Fig. 3. The response is nearly flat between 45 Hz to 10 kHz. In the low frequency range, the signal is gradually attenuated, and it gives approximately -30 dB at 3 Hz. For the high frequency part, the response is nearly flat up to 10 kHz. The frequency response can be taken into account in post processing.

MEASUREMENT OF THE PRESSURE FLUCTUATION FIELD IN A TURBULENT BOUNDARY LAYER

The microphone array has been applied to measurements in a turbulent boundary layer. A wind-tunnel of suction type with the test section size of 1.2 m $\times$ 0.8 m $\times$ 7.5 m has been used for the present experiment. The microphone array was placed at the center of the bottom wall and at 6.5 m from the beginning of the test section. The sampling period was set to 20 s for one experiment. The statistics were evaluated from this dataset.

The measurement has been undertaken at the free stream velocity U_e of 3 m/s. At the measurement location, the boundary layer thickness reaches approximately 140 mm, the friction velocity $u_\tau \sim 0.128$ m/s, the wall unit length $l^+ \sim 123$ μm. The friction Reynolds number $Re_\tau \sim 1140$. Under this condition, the diameter of the pressure hole normalized by the wall unit length $\phi^+ \simeq 4.1$, and the distance $\Delta x^+ \simeq 24.4$ and $\Delta z^+ \simeq 32.6$ The wall unit frequency f^+ defined as the inverse of the wall unit time t^+ is 1042 Hz.

To evaluate turbulent pressure fluctuations faithfully, undesired noise components should be removed from the measured data. Several noise reduction practices have been proposed: the subtraction method using auxiliary microphone mounted in the free stream capturing only the noise component (Naka *et al.*, 2006), and introducing Wiener filter to enhance the performance of the noise reduction (Naka *et al.*, 2015). Here, the POD mode analysis is used for the noise reduction to take advantage of the simultaneous measurements of 56ch fluctuating pressure signals. The first mode contributes 59% against the total power of fluctuation, and this mode has a large mean value in space indicating the perturbations having a long wavelength. Such fluctuations are attributable to the plane acoustic wave originating from the blower propagating in the mean flow direction.

Figure 4 represents the power spectra of the time fluctuating POD coefficients. The first mode exhibits peaky and noisy distributions. The shapes of the second and third modes are similar to the first mode in the higher and lower

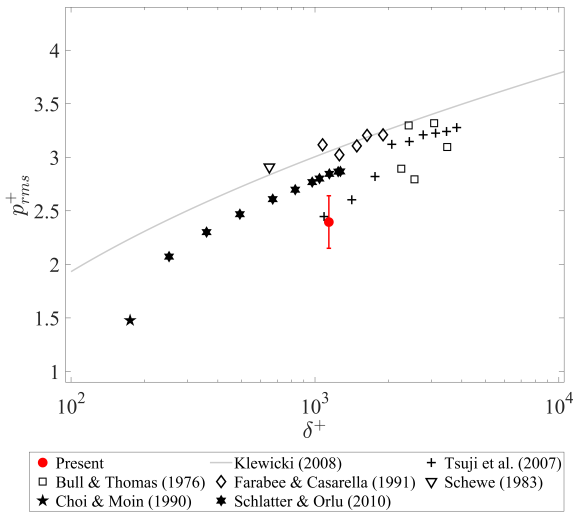

Figure 7. RMS of pressure fluctuations. Data are compared with the reference (Bull & Thomas, 1976; Schewe, 1983; Choi & Moin, 1990; Farabee & Casarella, 1991; Tsuji *et al.*, 2007; Klewicki *et al.*, 2008; Schlatter & Örlü, 2010).

frequency ranges, respectively. These corresponds to the noises in these frequency ranges. Furthermore, the noise in the higher frequency range more than 500 Hz is evident in the fourth mode. Here, therefore, the signals up to the fourth mode are considered to contain significant amount of noise. The turbulent wall pressure fluctuations are reconstructed from the 5th mode and the later. Figure 5 shows the cumulative sum of the energy in the POD modes. The first mode has 59% of the pressure fluctuations, and the POD modes after 5th mode possess approximately 30%. The contribution of the 5th mode is 1.2% and it gradually goes down to 0.36% for the 56th (final) mode.

Figure 6 indicates the consecutive space-time fluctuating pressure fields after noise treatment. It spans approximately 0.8δ in the spanwise direction, and $20\delta/U_c$ in time. The distributions clearly visualize the instantaneous structure of the wall pressure fluctuations. The negative and positive structures can be observed with a certain extent. The structures tend to spread more in the spanwise direction compared to the streamwise direction. This is consistent with the previous studies (Park & Moin, 2016). In addition, the wall pressure pattern is intermittent. The strong small scale fluctuation packets can be observed. Here, although the signals of adjacent microphones in span are slightly shifted in time considering the convection velocity of $U_c = 0.8U_e$, one still observes slightly jig-zag pattern. This can be inherent to the fact that the convection velocity is different for different size of structures.

The RMS value of the reconstructed wall pressure fluctuations normalized by the free stream velocity $p'/(\rho U_e^2)$ is 4.36×10^{-3}, which exhibits a good accordance with data in the literature (Schlatter & Örlü, 2010). The comparison of the wall pressure fluctuation is given in Fig. 7. In this comparison, the wall pressure fluctuations are normalized by the inner variables, and it is plotted against the wall unit boundary layer thickness δ^+. The present data are located in the trend of the data in the literature, but are situated slightly below. This may be attributed to the noise reduction procedure, where the first four POD modes are not considered. Though these POD modes apparently contains significant amount of noise, they possibly have some

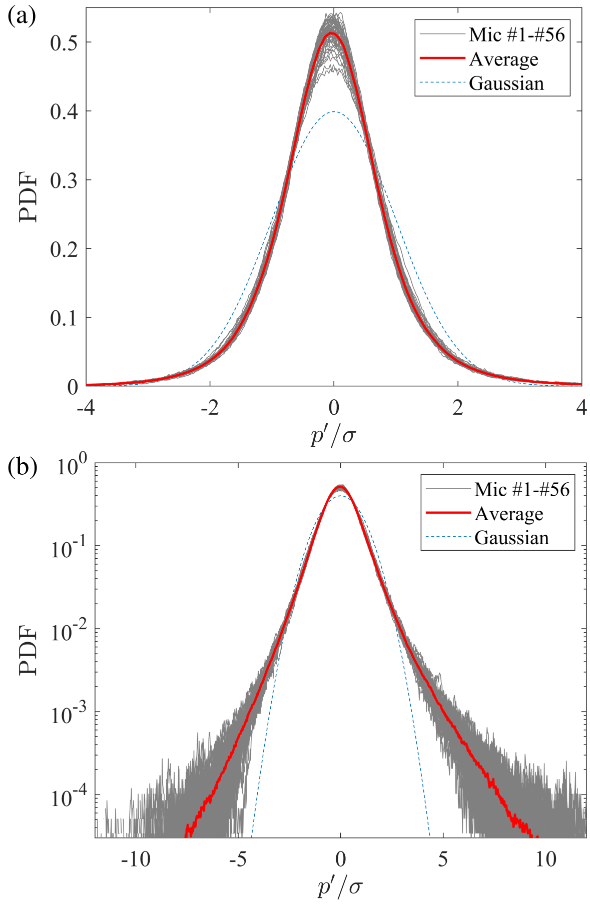

Figure 8. PDF of wall pressure fluctuations.

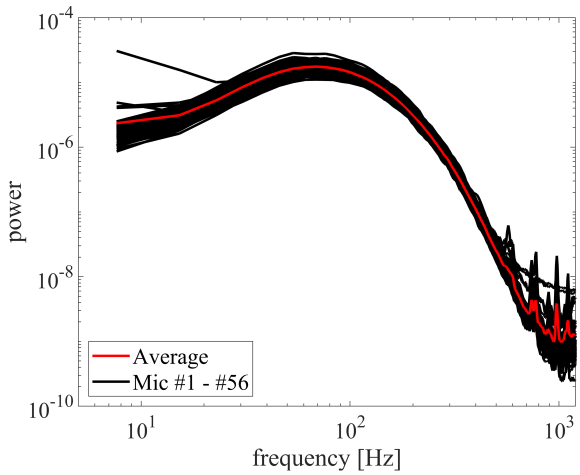

Figure 9. Power spectra of the wall pressure fluctuations from 56 microphones.

fractions of pressure fluctuations from the turbulent boundary layer. Another possible reason is estimation of the wall shear stress. Compared to the free stream velocity, it is not easy to determine the wall shear stress precisely. Here, the wall shear stress is obtained from the mean velocity profile measured using a hot-wire anemometer. The error-bar indicates the standard deviation of the 56 microphones. It is approximately 10% against the mean value.

Figure 8 presents the probability density functions (PDFs) of the wall pressure fluctuations. It is known that the

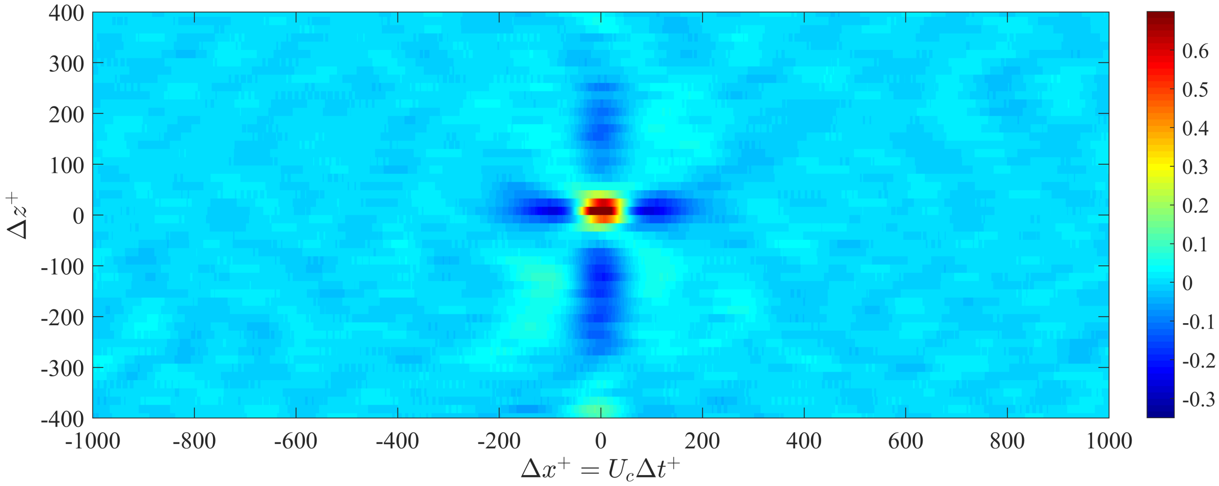

Figure 10. Normalized two-point cross correlation of the wall pressure fluctuation. The convection velocity $U_c = 0.8U_e$ is used for the time-space conversion.

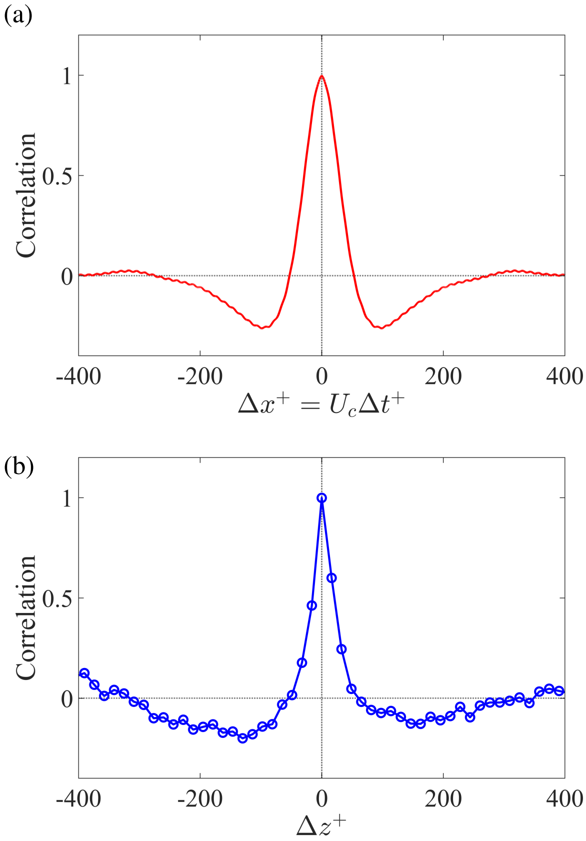

Figure 11. Normalized two-point cross correlation of the wall pressure fluctuation plotted along the lines of $\Delta z^+ = 0$ (a) and $\Delta x^+ = 0$ (b)

PDF of the wall pressure fluctuation is nearly symmetric on the contrary to the pressure fluctuations in the field (Tsuji *et al.*, 2007; Naka *et al.*, 2015). The profiles from 56 microphones are similar and the averaged line gives a smooth distribution down to 10^{-6}. The averaged value of the skewness is 0.40 and the flatness is 7.87. The PDF represents the intermittent nature of the pressure fluctuation and the shape is apparently broader than the Gaussian distribution.

Figure 9 indicates the power spectra of the reconstructed pressure fluctuations of 56 microphones. The profiles of the power spectra collapse well, and all the profiles smoothly decrease down to the wall unit frequency. It is noted that the hole diameter normalized by the wall unit length is $d^+ = 4.1$ and it gives far better spatial resolution than the value proposed in the literature (Gravante *et al.*, 1998) which suggests $d^+ < 18$ for the attenuation free measurement. In the low frequency part, the spectra is attenuated as it is observed in the frequency response shown in Fig. 3.

Figure 10 indicates the two-point correlation of the wall pressure fluctuations. It shows a meaningful pattern extending in the spanwise and streamwise directions. The distribution spreads broader in the spanwise direction than in the streamwise direction, which is the same tendency to the previous studies (Willmarth, 1975). Figure 11 shows the line plots along Δx and Δz directions. Both profiles are symmetric and show negative correlation from $53 \leq |\Delta x| \leq 275$ and $57 \leq |\Delta z| \leq 320$. In Δz direction, the significant level of negative correlation spreads further than in the Δx direction. The correlation crosses the value of -0.1 around 275^+ in Δz whereas 175^+ in Δx. Such difference can be explained by the turbulent flow structures above the wall. The simultaneous measurements with the velocity fields will reveal the instantaneous and statistical relationships between the wall pressure fluctuations and turbulent flow structures.

CONCLUSION

In the present study, a microphone array is designed for the wall pressure fluctuation measurement. 56 MEMS digital microphones are controlled by a FPGA board. The output of the microphones is calibrated against the reference microphone to obtain the actual pressure fluctuation in Pascal. The microphone array is placed in the wind tunnel and the pressure fluctuations in a turbulent boundary layer are measured. The background noise in the raw data is well treated by POD mode analysis taking advantage of the simultaneously measured 56ch data. The RMS values of obtained pressure fluctuations are in good accordance with the data in the literature. In addition, the power spectra exhibit smooth shape up to the wall unit frequency.

It is confirmed that the present method provides a novel flexible method for measuring wall pressure fluctuations with a good spatial and temporal resolutions. The time resolved fluctuating wall pressure fields give experimental insights of the relationship between the wall pressure fluctuation pattern and the wall turbulence structures.

The present microphone array can be synchronized with other microphone arrays or devices by external triggering. The extension of the present method to a massively parallel fluctuating pressure measurement system is possible.

ACKNOWLEDGEMENT

This work was supported by JSPS KAKENHI Grant-in-Aid for Young Scientists (B) Grant Number JP16K18010.

REFERENCES

Bull, M. K. & Thomas, A. S. W. 1976 High frequency wall-pressure fluctuations in turbulent boundary layers. *Physics of Fluids* **19** (4), 597–599.

Choi, H. & Moin, P. 1990 On the space-time characteristics of wall-pressure fluctuations. *Physics of Fluids* **2** (8), 1450–1460.

Farabee, T. M. & Casarella, M. J. 1991 Spectral features of wall pressure fluctuations beneath turbulent boundary layers. *Physics of Fluids* **3** (10), 2410–2420.

Gravante, S. P., Naguib, A. M., Wark, C. E. & Nagib, H. M. 1998 Characterization of the pressure fluctuations under a fully developed turbulent boundary layer. *AIAA Journal* **36** (10), 1808–1816.

Klewicki, J. C., Priyadarshana, P. J. A. & Metzger, M. M. 2008 Statistical structure of the fluctuating wall pressure and its in-plane gradients at high Reynolds number. *Journal of Fluid Mechanics* **609**, 195–220.

Matsubara, M., Sendai, Y., Matsumoto, K. & Mishiba, T. 2014 Influence of tripping on spatiotemporal correlation between velocity and wall pressure in a turbulent boundary layer. In *Progress in Turbulence V*, pp. 103–106.

Naka, Y., Omori, T., Obi, S. & Masuda, S. 2006 Simultaneous measurements of fluctuating velocity and pressure in a turbulent mixing layer. *International Journal of Heat and Fluid Flow* **27** (4), 737–746.

Naka, Y., Stanislas, M., Foucaut, J.-M., Coudert, S., Laval, J.-P. & Obi, S. 2015 Space–time pressure–velocity correlations in a turbulent boundary layer. *Journal of Fluid Mechanics* **771**, 624–675.

Park, G. I. & Moin, P. 2016 Space-time characteristics of wall-pressure and wall shear-stress fluctuations in wall-modeled large eddy simulation. *Physical Review Fluids* **1** (2), 024404.

Schewe, G. 1983 On the structure and resolution of wall-pressure fluctuations associated with turbulent boundary-layer flow. *Journal of Fluid Mechanics* **134**, 311–328.

Schlatter, P. & Örlü, R. 2010 Assessment of direct numerical simulation data of turbulent boundary layers. *Journal of Fluid Mechanics* **659**, 116–126.

Tsuji, Y., Fransson, J. H. M., Alfredsson, P. H. & Johansson, A. V. 2007 Pressure statistics and their scaling in high-Reynolds-number turbulent boundary layers. *Journal of Fluid Mechanics* **585**, 1–40.

White, R., Krause, J., De Jong, R., Holup, G., Gallman, J. & Moeller, M. 2012 MEMS microphone array on a chip for turbulent boundary layer measurements. In *50th AIAA Aerospace Sciences Meeting including the New Horizons Forum and Aerospace Exposition*, p. 260.

Willmarth, W. W. 1975 Pressure fluctuations beneath turbulent boundary layers. *Annual Review of Fluid Mechanics* **7**, 13–36.